Supporting Information for "Variability in the global ocean carbon sink from 1959-2020 by correcting models with observations"

Val Bennington[1,2], Lucas Gloege[3], Galen A McKinley[1]

[1]Columbia University and Lamont-Doherty Earth Observatory New York, USA

[2]Makai Ocean Engineering, Inc., Hawaii, USA

[3]NASA-GISS, New York, USA

Contents of this file

1. Text S1-S4

2. Figures S1-S4

Corresponding author: Val Bennington, Makai Ocean Engineering, Inc. Hawaii, USA. (Valerie.Bennington@makai.com)

S1. Model-Data Misfits by Season

Figure S1 shows the reconstructed model-data misfits by season for each of the eight GOBMs. These misfits are reconstructed globally and at all times by the machine learning algorithm.

S2. Model-Adjusted CO_2 Fluxes

Figure S2a depicts the annual anthropogenic air-sea CO_2 flux estimated by each of the uncorrected GOBMs. After model-data misfits are reconstructed and applied, corrected model air-sea $CO2_2$ fluxes are shown in Figure S2b for each of the eight GOBMs. Figure S2c shows the corrections applied to each of the model air-sea CO_2 fluxes. This correction includes the riverine efflux adjustment of 0.49 PgC/yr.

S3. Reconstructed Air-Sea CO_2 Fluxes

Figure S3 shows the air-sea CO_2 fluxes reconstructed by LDEO-HPD as compared to the eight GOBMs and HPD Climatology Test (Figure S3a), Jena MLS (Figure S3b), other observation-based products (Figure S3c) and the box model simulations with and without volcanoes (McKinley et al., 2020) (Figure S3d).

S4. Anomalies of Detrended Reconstructed Air-Sea CO_2 Fluxes

Figure S4 shows the anomalies of detrended air-sea CO_2 fluxes in the four ocean basins. The years of major volcanic eruptions are depicted with vertical grey lines Agung (1963), El Chichon (1982) and Mt. Pinatubo (1991). The Pacific and Southern Oceans show

clear increases in their ocean sink immediately following the volcanic eruptions.

References

McKinley, G. A., Fay, A. R., Eddebbar, Y. A., Gloege, L., & Lovenduski, N. S. (2020). External forcing explains recent decadal variability of the ocean carbon sink. *AGU Advances*, *1*(2), e2019AV000149. doi: https://doi.org/10.1029/2019AV000149

Rödenbeck, C., DeVries, T., Hauck, J., Le Quéré, C., & Keeling, R. (2021). Data-based estimates of interannual sea–air co_2 flux variations 1957–2020 and their relation to environmental drivers. *Biogeosciences Discussions*, *2021*, 1–43. doi: 10.5194/bg-2021-304

Figure S1. Reconstructed model-data misfit by season for each of the eight GOBMs used. (μatm)

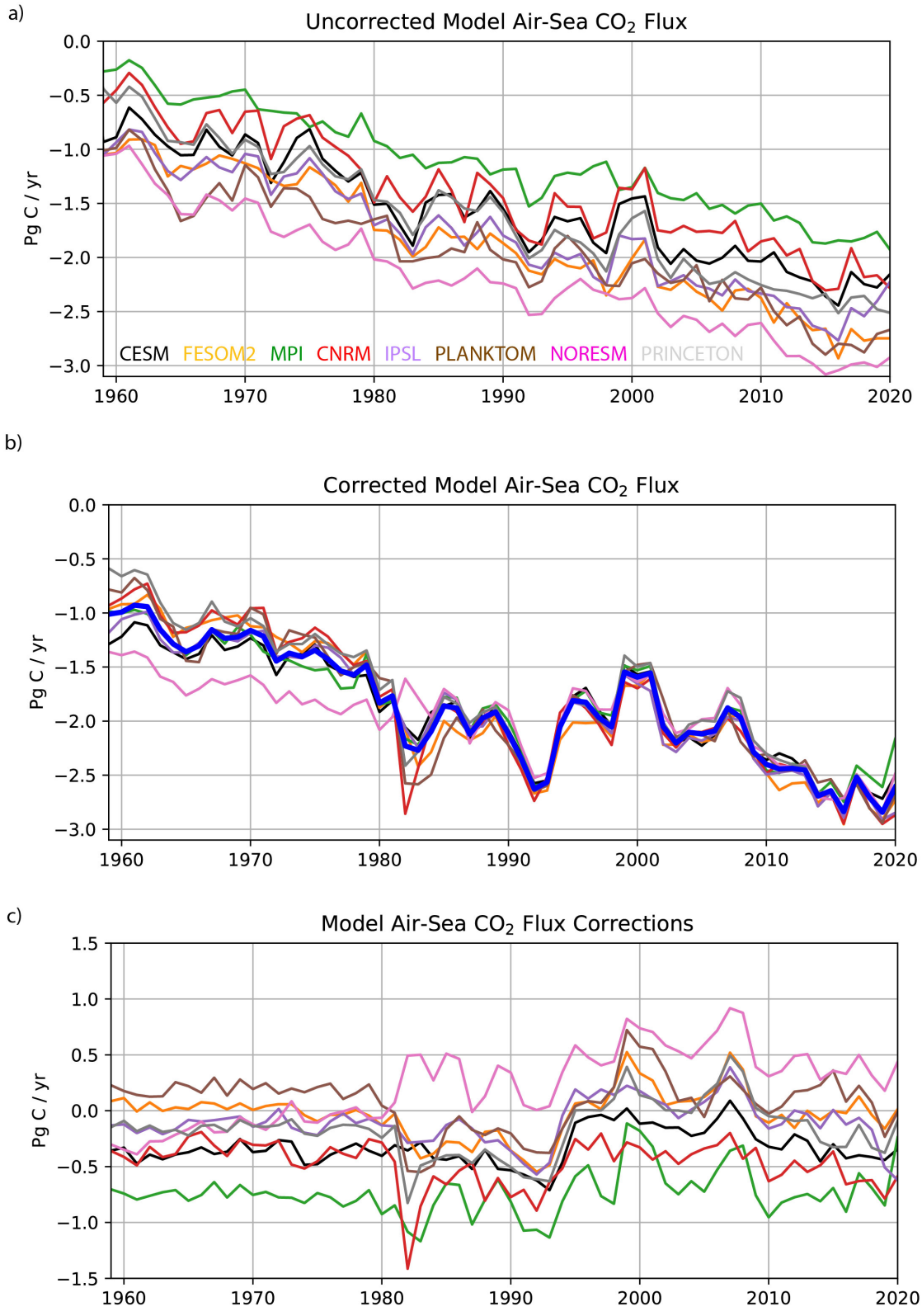

Figure S2. Model anthropogenic CO_2 Flux (Pg/C/yr) for each of the eight GOBMs before (a) and after (b) model-data misfits are applied. Corrections to each model are shown in (c). Riverine carbon efflux corrections are used in (b) and (c). Riverine carbon efflux assumed to be 0.49 Pg/C/yr, as described in Methods, such that the mean model result (dark blue) is identical to Figure 3a.

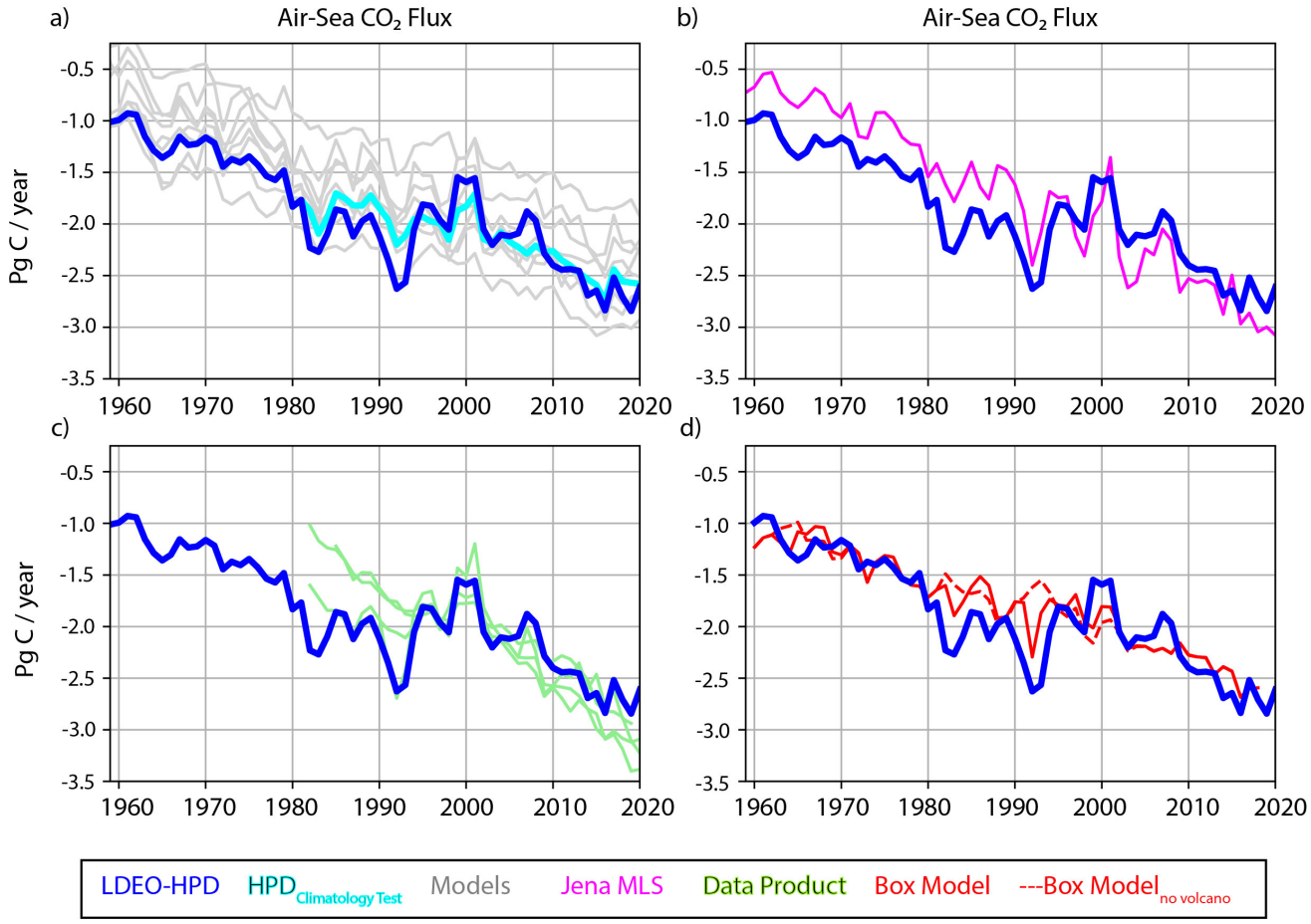

Figure S3. (a) Air-sea CO_2 fluxes for 1959-2020 according to LDEO-HPD (blue), HPD Climatology Test (cyan), and the eight unadjusted GOBMs (grey). (b) Air-sea CO_2 fluxes for 1959-2020 according to LDEO-HPD (blue) and Jena MLS (magenta) (Rödenbeck et al., 2021). (c) Air-sea CO_2 fluxes for 1959-2020 according to LDEO-HPD (blue) and the other data products (green). (d) Air-sea CO_2 fluxes for 1960-2018 according to LDEO-HPD (blue) and the box model of McKinley et al. (2020) with volcanoes (red) and without volcanoes (dashed red).

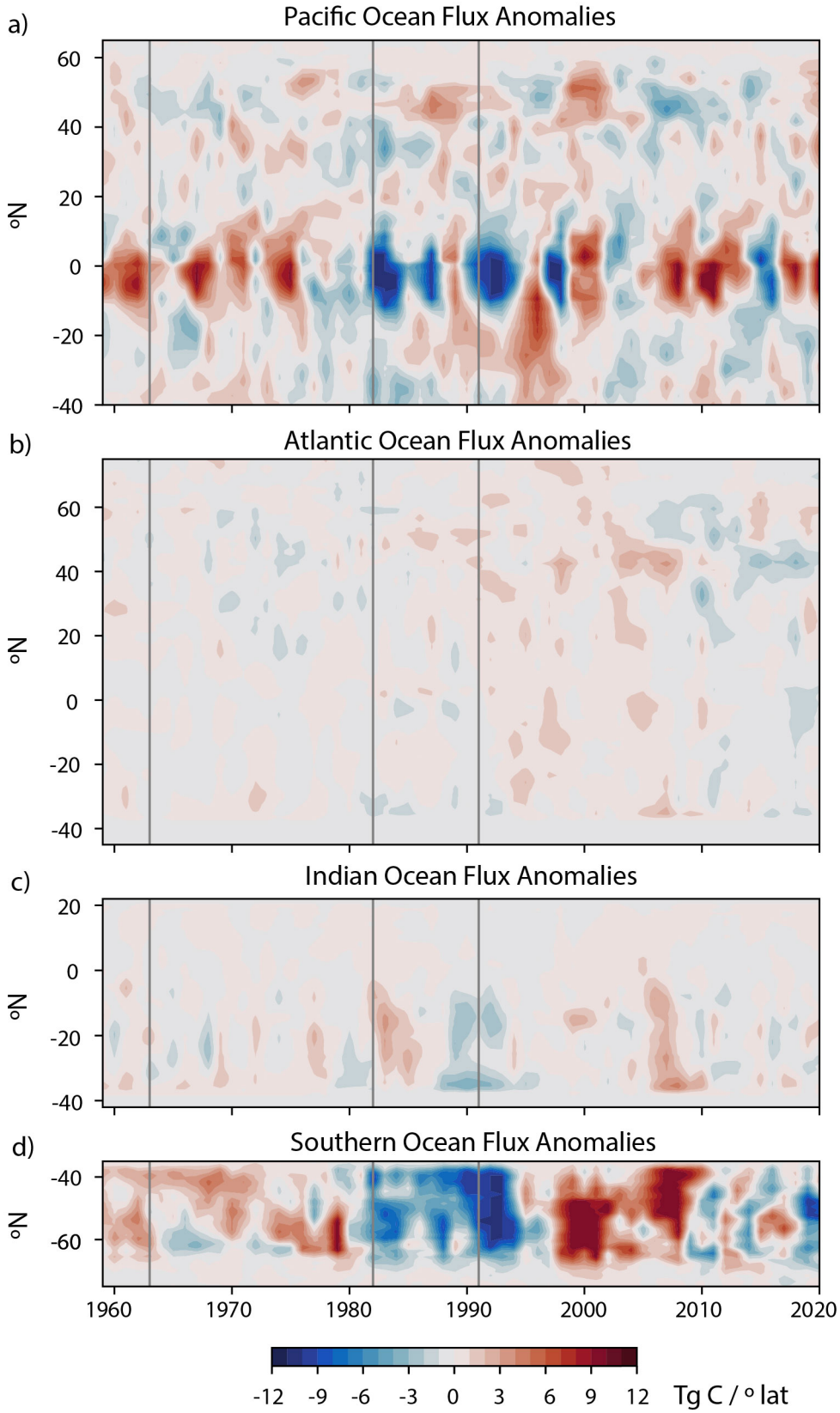

Figure S4. Detrended air-sea CO_2 flux anomalies in four ocean basins (TgC/yr/^{o}lat). Major volcanic eruptions denoted with vertical grey lines (Agung, March 1963; Chichon, April 1982; Pinatubo, June 1991).